Proceedings World Geothermal Congress 2020+1
Reykjavik, Iceland, April - October 2021

Geothermal, Tectonic, and Magmatic Stress Interactions in the Hengill Area, Iceland

Halldór Geirsson, Cécile Ducrocq, Hanna Blanck, Thora Ánadóttir, Kristín S. Vogfjörd, Bjarni Reyr Kristjánsson, Gunnar Gunnarsson, Vala Hjörleifsdóttir, Daniel Juncu, Freysteinn Sigmundsson, Benedikt G. Ófeigsson, Vincent Drouin

Nordic Volcanological Center, Institute of Earth Sciences, University of Iceland, Sturlugata 7, 101 Reykjavík, Iceland

Corresponding author: hgeirs@hi.is

Keywords: Deformation, subsidence, crustal stress, Hengill, process interactions

ABSTRACT

Geothermal production, including fluid extraction and re-injection, causes permanent changes in crustal stresses and fluid pressures, which affect nearby seismicity and fault movements. Stress changes can in general also affect magmatic movements, such as dike propagation, dike arrest, and formation and growth of magma chambers. Here, we use the Hengill area in SW-Iceland as a natural laboratory to study study stress and fluid interactions of geothermal, tectonic, and magmatic processes.

Hengill has been subject to various geological events in the past decades. In addition to the ~1.9 cm/yr of plate motion across the Hengill area, during 1994 to 1998 an intrusion caused uplift of about 8 cm in the Eastern part of the Hengill area and triggered nearly one hundred thousand of earthquakes with the largest one of magnitude 5.5. From the end of 1999 until 2006 the area was relatively quiet. In 2006 the Hellisheiði geothermal powerplant commenced and the Nesjavellir powerplant was enlarged, leading to a combined 420 MW electricity and 430 MW hot water produced in the Western part of the Hengill area. Localized subsidence of up to ~2.5 cm/yr is observed in the main production areas, however, temporary inflation was observed in the main injection area in 2011-2012. In 2006 widespread subsidence started in the Eastern part of the Hengill area, inferred to originate from about 7 km depth, similar to the intrusion in the nineties. This subsidence now amounts to at least 12 cm total, far exceeding the inflation in the nineties. In late 2017, the Eastern-Hengill subsidence temporarily changed to inflation, but subsidence resumed in the spring of 2018. These deep inflation-deflation episodes link to the energy recharge processes of the geothermal systems, whether magma or hydrothermal fluids dominate the deformation process. In 2016 geothermal production started from a part of the Hengill area called Hverahlíð, a few km SE of the main production area. We observe small deformation in this region, in rough agreement with the relative geothermal fluid mass outtake in the area.

The deformation data provides a comprehensive description of ongoing processes and we have, for example, used it to generate time-dependent surface strain maps and constrain key reservoir parameters such as depth of pressure change, reservoir recharge, steam ratio and reservoir bulk modulus. We compute simple models of stress changes from idealized geothermal areas. The stress changes imposed by the geothermal production are found to have widespread effects, both in terms of earthquake triggering and dike propagation.

1. INTRODUCTION

The existence of geothermal resources is a result of magmatic, tectonic and hydrothermal processes: heat from intruded magma cools down with hydrothermal heat mining via tectonic fractures in the rock (e.g., Stimac et al., 2015). However, many of these processes depend on each other (Figure 1). Magmatic intrusions cause earthquakes and fault movement, that again change the ways water travels in the crust. Tectonic stresses and faulting due to plate motion changes stresses and affects where magma accumulates or where dikes form. The buildup of the Earth's crust through intrusions, eruptions, and sedimentary processes, causes mechanical layering that affects the way that future dikes travel (Gudmundsson et al., 2006). In a similar way, stress changes caused by geothermal production affect seismicity, faulting, and pathways of future dikes in their surroundings. Here we will review the different types of stress interactions, with special emphasis on the Hengill area.

The Hengill volcanic system (Figure 2) hosts the high-temperature Nesjavellir and Hellisheiði geothermal power-plants with a combined production of 420 MW electricity and 430 MW hot water. Hengill is located at a triple-junction in the plate boundary system across Iceland (Sigmundsson et al., 2018). The North-American (NA) and Eurasian (EU) plates are diverging at a total rate of 1.8 cm/yr in Iceland (e.g., Geirsson et al., 2006), however, the NA-EU divergence is split between the Western and Eastern Volcanic Zones of Iceland (WVZ and EVZ, respectively; Figure 1). The resulting tectonic microplate between the WVZ and EVZ is called the Hreppar block (Einarsson, 1991). Currently, most of the plate spreading is taken up at the EVZ. Sigmundsson et al. (1995) used GPS measurements to estimate that only 15% +- 15% of the plate spreading is taken up in the EVZ, while Árnadóttir et al. (2009), using a more extensive GPS data set and a different kind of modelling, estimated about 30% of the total plate motion to be taken up at the WVZ. LaFemina et al. (2005) proposed a model consistent with propagating Mid Ocean Ridges, where the opening rate on the WVZ decreases from south to north, and increases from the south to north along the EVZ, conserving the total EU-NA plate motion. The current geographic location of the center of the triple junction is somewhat uncertain, by perhaps 10 km, as reported by Árnadóttir et al. (2009), Travis (2012), and Geirsson et al. (2012). The surface expression of the tectonic movements in the Hengill area are various fault structures, strike-slip faults, normal faults, and eruptive fissures (Steigerwald et al., 2018).

Hengill has been subject to various geological events in the past decades. Plate motion causes steady build-up of strain and intermittent earthquakes releasing that strain. In 2008 two M6.1 earthquakes occurred just east of the area on N-S trending vertical strike-slip

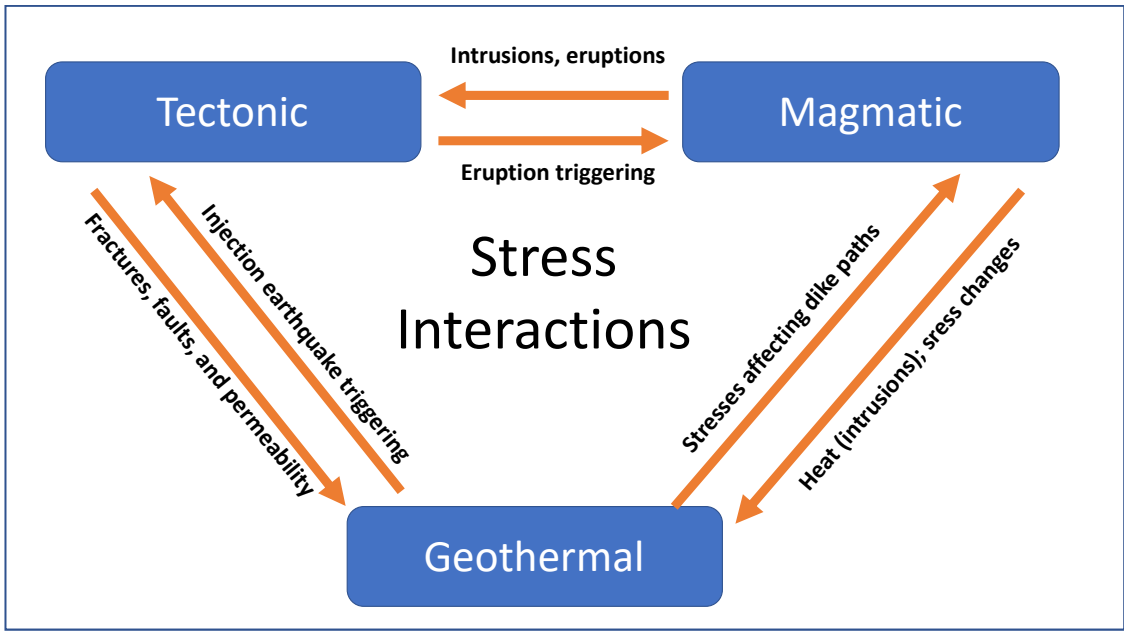

Figure 1: Schematic overview of selected stress-based interactions of geothermal, tectonic, and magmatic processes.

faults (Hreinsdóttir et al, 2009; Decriem et al., 2010), as typical for the largest earthquakes occurring in the South Iceland Seismic Zone and the Hengill area (Einarsson, 1991). During 1994-1998 an intrusive episode at about 7 km depth in the eastern part of the Hengill area caused 2 cm/yr of uplift and tens of thousands of earthquakes, including several M>5 events (Sigmundsson et al., 1997; Feigl et al., 2000). Since 2006 to at least 2019, widespread subsidence has prevailed in the eastern part of the Hengill area (Geirsson et al., 2010; Juncu et al. 2017; Árnadóttir et al., 2018), modelled by Juncu et al. (2017) to be at a similar depth (~7 km) as the 1994-1998 inflation source, but offset by about 3 km to the NW. Árnadóttir et al. (2018) suggest that the subsidence triggered the M6.1 earthquake doublet. The latest event in the Hengill area is a short-lived inflation event during 2017-2018, centered at 5-9 km depth in the east of the area, near the 2006-present subsidence center (Ducrocq et al., 2019). Thus, although the Hengill volcanic system has not erupted on the surface in the past 2000 years, it is far from being volcanically inactive.

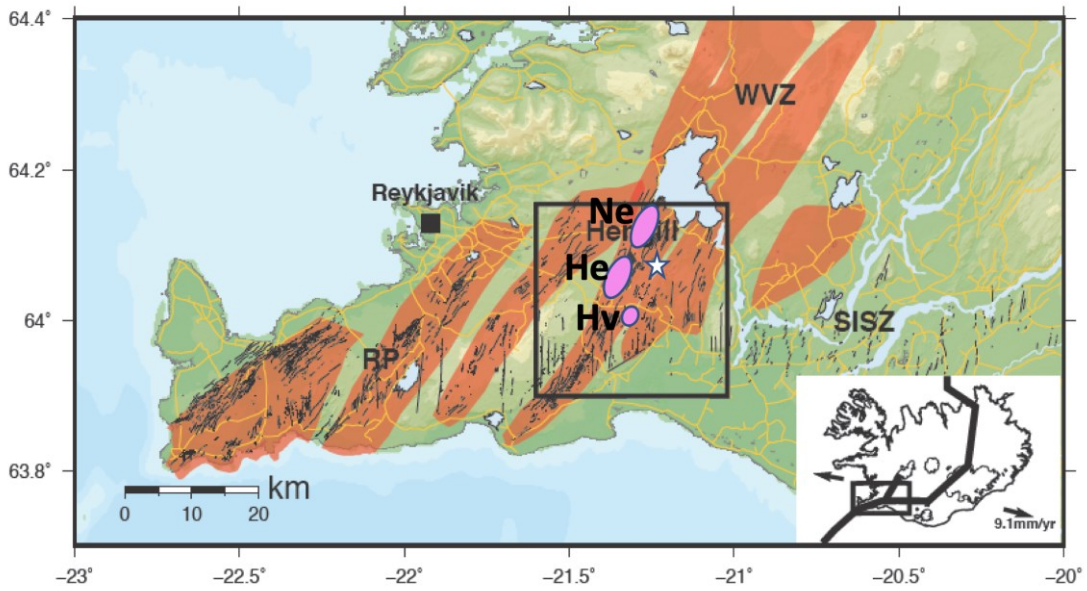

Figure 2: Overview of the Hengill area. The pink areas, He, Ne, and Hv refer to the geothermal production areas Hellisheiði, Nesjavellir, and Hverahlíð, respectively. Orange areas show outlines of fissure swarms for the volcanic systems. White star shows location of the 2006-present Ölkelduháls subsidence. Inset shows the EU-NA plate boundary in Iceland (thick lines) and box shows outline of main figure. [Figure from Juncu et al. 2017].

Geothermal energy production causes pressure and temperature decrease in the reservoir, which results in measurable crustal subsidence at the surface. Although geothermal production started in Nesjavellir in 1990, its production was greatly increased in 2006, at a similar time as the larger Hellisheiði powerplant commenced. The maximum subsidence rate over the Hellisheiði reservoir is ~2.5 cm/yr, and ~1.5 cm/yr at Nesjavellir (Juncu et al., 2017; Figure 3). A new production area commenced in 2016 in Hverahlíð, around 3 km SSE of the center of the Hellisheiði production area (Figure 1). However, the rate of geothermal fluid mass extraction at Hverahlíð is but a fifth of the extraction rate at Hellisheiði. Wastewater fluid injections near the Hellisheiði power plant have caused significant seismicity, including M~4 events that were widely felt in SW Iceland (Bessason et al., 2012). Accompanying the onset of the injection in Húsmúli (2 km NNW of the Hellisheiði power plant) in 2011, a transient uplift episode was observed in Húsmúli (Juncu et al., 2018).

All these deformation events change the state of stress in the crust, affecting nearby seismicity, fault movements, and crustal fluid flow.

2. DEFORMATION FIELD OF THE HENGILL AREA

Plate motion dominates the horizontal component of the crustal deformation field in the Hengill area (Juncu et al., 2017). The plate boundary deformation area spans several tens of kilometers perpendicular to the plate boundary axis, as the motion gradually approaches the NA or EU plate motion on either side of the plate boundary axis. Earthquakes release some of the gradual plate boundary strain build-up. It has been proposed that we are in the middle of an earthquake sequence in the South Iceland Seismic Zone (SISZ): the 2000-2008 earthquakes released only about half of the elastic energy built up since the previous earthquake sequence in 1896-1912 (Decriem et al., 2010). Typically, we do not have resolution to measure permanent surface deformation from earthquakes smaller than approximately 4-4.5 in magnitude. Several earthquakes larger than M4.5 have occurred in and bear the Hengill area in recent decades. The largest earthquakes in the SISZ, Hengill, and Reykjanes are strike-slip events on N-S trending vertical right-lateral faults. The 1994-1998 unrest episode culminated with earthquakes of magnitude 5.4 and 5.1 in the Hengill area in June and November 1998, respectively (Vogfjörd and Slunga, 2003; Jakobsdóttir, 2008). In June 2000, two M6.5 earthquakes occurred further east in the South Iceland Seismic Zone (REF). The former M6.5 event dynamically triggered several M>5 earthquakes in the Reykjanes and Hengill areas (REFs). For earthquakes larger than approximately M6 we can expect some form of post-seismic motion, in addition to the co-seismic deformation, lasting for months to decades. Significant post-seismic deformation was observed for the June 2000 earthquakes (Jónsson et al., 2003; Decriem and Árnadóttir, 2012). In May 2008 the east part of the Hengill area was struck by two M6.1 earthquakes. Between 2009 and 2019, the largest earthquakes to occur in the Hengill area were the M4 events in October 2011, associated with the injection in Húsmúli (Bessason et al., 2012; SIL catalog).

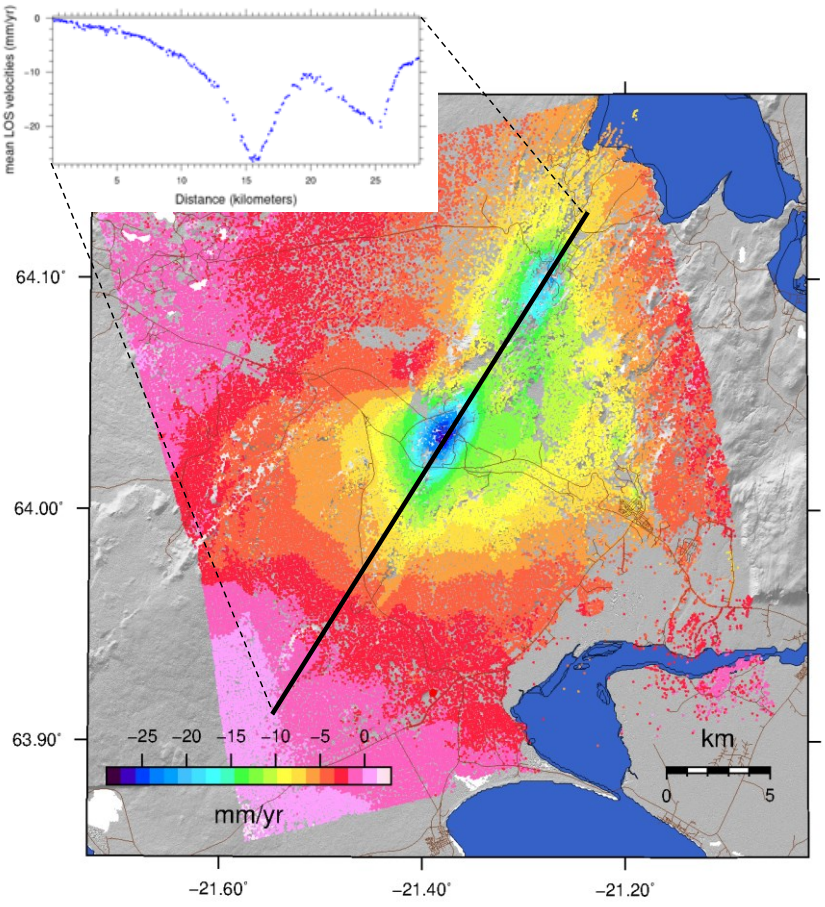

Figure 3: Mean line-of-sight (close to vertical) velocity field 2009-2017 using the TerraSAR-X satellite. Plate motion has been removed from the data for clarity. Subsidence is centered on the main production areas. Inset figure shows deformation along a profile from SSW to NNE, crossing the Hellisheiði and Nesjavellir subsidence centers.

To study the current deformation in the Hengill area, we used Interferometric Synthetic Aperture Radar (InSAR) data from the German Space Agency's (DLR) TerraSAR-X satellite. We used 20 images for our study from the ascending track 41 (heading 346°, right-looking, look-angle between 26 to 42°) of the satellite spanning 2009-10-22 to 2017-09-23. Using the DORIS software (Kampes et al., 2003), we processed 64 interferograms between pairs of images selected specially to have small perpendicular and temporal baselines, according to the small baselines method implemented in the StaMPS software (Hooper et al., 2008; 2012). Topographic corrections were calculated (Kampes et al., 2003, Massonet et al., 1995) using an intermediate resolution (25 m) digital elevation model from the TanDEM-X mission. The multitemporal approach from the StaMPS software allows us to increase the number of pixels that are spatially coherent throughout our interferograms, and to estimate an average line-of-sight (LOS) velocity for each pixel during our period of study (Hooper et al., 2012). Sixteen of our interferograms had to be eliminated from the time series due to large atmospheric perturbations. The resulting mean LOS velocity map is referenced to a small area at the coordinates 21.3897°W 63.9211°N. The InSAR data is primarily sensitive to vertical deformation, but horizontal (mostly east-west) deformation is also picked up by the satellites. We correct for plate motion in the area by applying the plate boundary model of Árnadóttir et al. (2009). The resulting volcanic and geothermal deformation (Figure 3) is visually dominated by three subsidence centers: at Hellisheiði, Nesjavellir, and Ölkelduháls, as described by Juncu et al. (2017) using data from the same satellite during 2012-2015. We note that the subsidence signals from Hellisheiði and Nesjavellir partially overlap (Figure 3, inset). The deformation signals from the Hellisheiði and Nesjavellir production areas are narrow, caused by shallow (1-2.5 km) deformation sources - i.e., the geothermal reservoir - superimposed on the wider Ölkelduháls signal caused by a ~7 km deep deformation source (Juncu et al., 2017; 2019). The visual extent of the deformation signal associated with the geothermal productuin is not a good measure of the size of the geothermal reservoir: the visible size of the signal depends on the signal-noise ratio, and hence increases year by year as more data is acquired and the total signal gets larger.

3. STRESS INTERACTIONS

Rocks do typically not stretch or deform very easily, i.e., it takes high stresses to deform rocks. From Hooke's law, this means that the elastic moduli of rocks are high, typically some tens of giga-Pascals (GPa). Likewise, as a result of Hooke's law, small strains will cause high stresses in rocks. Below we review several modes of stress interactions most relevant to geothermal areas. For magma-tectonic interactions, the reader is referred to several published studies (e.g., Acocella et al., 2014; Sigmundsson et al., 1997; Nostro et al., 1998; LaFemina et al., 2004; LaFemina 2015).

3.1. Tectonic-geothermal interactions

Tectonic forces stress rocks to failure, causing faulting in the crust. The faults facilitate more efficient fluid flow than through unbroken rock matrix, one of the key ingredients for a geothermal system. Faulting leads to dual-permeability materials, where some of the flow properties are controlled by the fractures, while others (e.g. total energy content) are controlled by the less permeable rock matrix. But all interactions work both ways. Production in geothermal areas affects tectonic processes primarily by two means: a) changes in fluid pressure due to fluid extraction and injection, and b) changes in crustal stresses due to deformation of the geothermal reservoir. Both of these affect triggering of earthquakes.

Earthquake triggering is most readily described by changes in Coulomb Failure Stress (CFS), $\Delta\sigma_{CS}$:

$$\Delta\sigma_{CS} = \Delta\tau + \mu(\Delta\sigma_N + \Delta p), \quad (1)$$

where $\Delta\tau$ notes change in shear stress (positive if parallel to fault slip vector), $\Delta\sigma_N$ notes the change in normal stress (positive for less normal stress), Δp notes the change in pore pressure, and μ is the coefficient of friction on a receiver fault that has a given strike, dip, and rake (Harris and Simpson, 1992). A positive change in CFS brings receiver faults closer to failure, i.e. has potential to trigger pre-loaded faults, and a negative change in CFS brings a fault further from failure. Wastewater fluid injections thus bring all fault orientations closer to failure, while fluid extractions tend to bring faults further from failure (Equation 1; Ali et al., 2016) The change in reservoir fluid pressure is sometimes taken as in-situ measurements of change in pressure in boreholes, although liquid-steam phase change caused by the pressure change can complicate matters. To study stress changes outside the reservoir we can ignore Δp, or assume it is proportional to change in normal stress, and rewrite Equation 1 as

$$\Delta\sigma_{CS} = \Delta\tau + \mu'\Delta\sigma_N, \quad (2)$$

where μ' is called the effective coefficient of friction. In general we do not know well the friction coefficient; it must change with location and time along faults. Hence, ad-hoc values of μ'equal 0.4 to 0.8 are commonly used (Toda et al., 2011).

To simulate stress changes from geothermal production, we used the Coulomb 3.3 software (Toda et al., 2011) to calculate CFS for a hypothetical geothermal reservoir centered at 2 km depth in a uniform elastic half space and disregarding the effect of fluid discharge, i.e. the solution is primarily valid outside the reservoir. We assume an effective coefficient of friction of 0.4, and a net source volume change of -2.1 x 10^5 m^3/yr, similar to what is observed for the Hellisheiði production area (Juncu et al., 2019). Note that this volume change does not equal the extraction volume for production; it is the effective net volume decrease of the reservoir including extraction, reservoir recharge and reservior phase changes, deduced from models of the surface deformation (Juncu et al., 2019). We choose here to calculate the CFS for N-S trending vertical right-lateral strike-slip faults because the largest earthquakes in south Iceland occur on these faults. The resulting change in CFS (Figure 4a) shows a quadrantal pattern where CFS is increased NW and SE of the production area, while CFS is lowered towards the SW and NE quadrants. A north-south cross-section across the CFS changes, offset 1.5 km east of the reservoir, reveals that each N-S trending fault has both positive and negative changes in CFS, such that the net CFS is close to zero. The affected volume is mostly above the central depth of the reservoir. For stress triggering thresholds of earthquakes, values of 0.1 bar (10 kPa) are often cited (Stein, 1999). It is interesting to note that because the geothermal deformation is ever ongoing, the geographic extent of the affected area grows continually: after 1 year the triggering threshold extends to ~5 km from the source (Figure 4), after 10 years it extends to ~10 km, and after 100 years of production the 0.1 bar threshold is at ~25 km from the subsidence center for this particular example. Eventually, the crust closest to (or within) the reservoir will be strained to failure, inducing (as opposed to triggering - see Dahm et al. (2015)) it's own small earthquake (Im et al., 2017). The induced

earthquake will be relatively small because the crustal deformation from a source at 2 km depth is quite limited in space, but may potentially alter fluid flow in the reservoir (Im et al., 2017) or trigger larger earthquakes on nearby faults. Further work will study CFS on different fault orientations and relation to relative earthquake relocation, fault mapping and seismic inference of sense of slip from microearthquakes (Blanck et al., 2019).

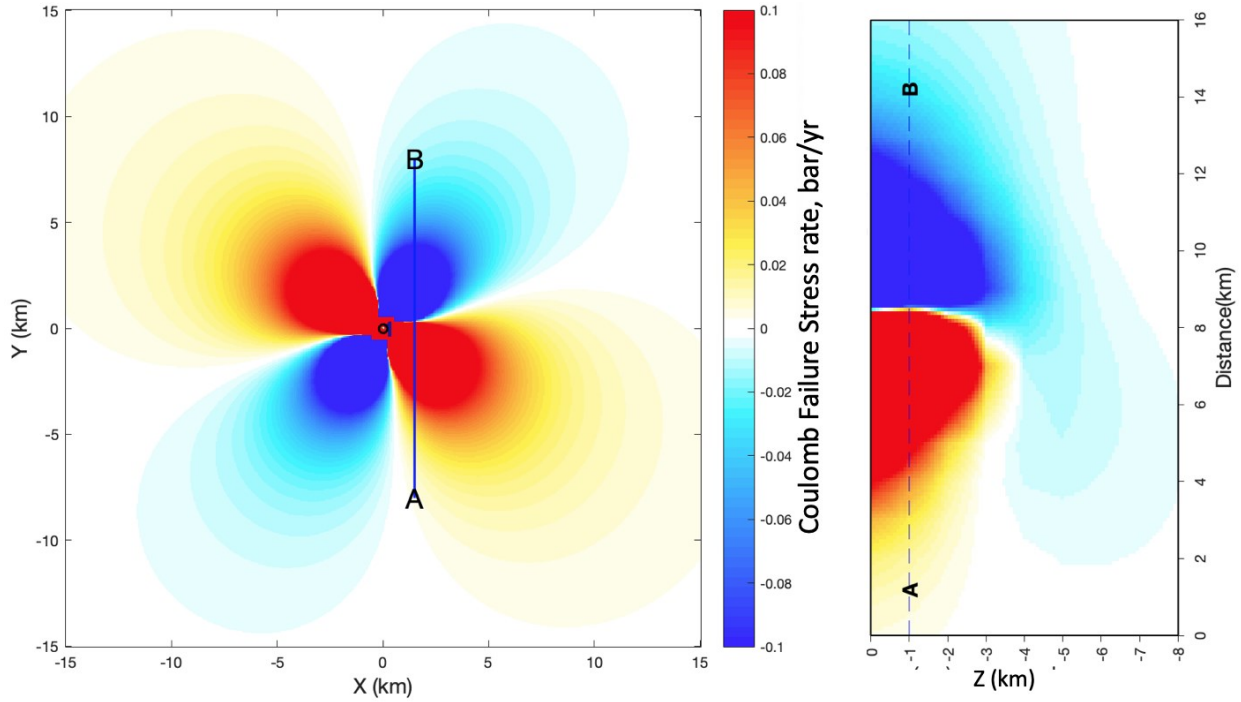

Figure 4: Coulomb Failure Stress rate, in bar/yr, for a deflating point-source located at 2 km depth. Left: Depth-section at 1 km depth. Right: Cross-section A-B as indicated on left figure. The color scale is set to saturate at 0.1 bar/yr.

3.2. Magma-geothermal interactions

The magmatic origin of high-temperature geothermal systems is obvious. Magmatic intrusions cool off over thousands of years, giving rise to multi-phase fluid-driven heat transport and creating geothermal systems. It is, however, not well known if the heat source comes from a series of sheet-like intrusions or from a single (or episodically repeated) "batholithic" intrusion at the right depth to form geothermal systems that can be economically harnessed.

The reverse interaction; how geothermal systems can affect magma transport in the crust, is also of interest. The subsidence associated with pressure and temperature changes in the geothermal reservoir causes stress changes that affect paths of dikes and likelihood of stalling propagating dikes to form intrusive bodies. The problem is to a first degree computationally identical to a cooling magma chamber, with the same shape as the reservoir. Dike paths are primarily affected by normal stresses, and here we calculate normal stress changes due to a source with the same depth and volume characteristics as in Section 3.1. We calculate the stresses for optimally oriented faults in a crust free of external (tectonic) stresses (Toda et al., 2011). The resulting pattern of normal stress change has a cylindrical symmetry. Closest to the source (we assume a very small source here), above it and below it, compression, i.e. negative unclamping, dominates the stress changes (Figure 5). Further away, the crust is dilated and positive unclamping dominates. Below about double the source depth, directly under the source, there is slightly positive unclamping, while slightly negative outside the central area. This pattern would tend to focus dikes towards under the center of the geothermal production area at depths below approximately 4-6 km depth. The dikes would have a tendency to stall at this depth due to a small stress barrier (Figure 5). Our simple model indicates that if the dikes make it past the stress barrier to shallower depths, then the tendency will be to deflect them to the sidea of the production area. However, we note that the dominating tectonic and lithostatic stresses (i.e. topography and density differences - e.g. Sigmundsson et al. (2014)) should be considered for further studies.

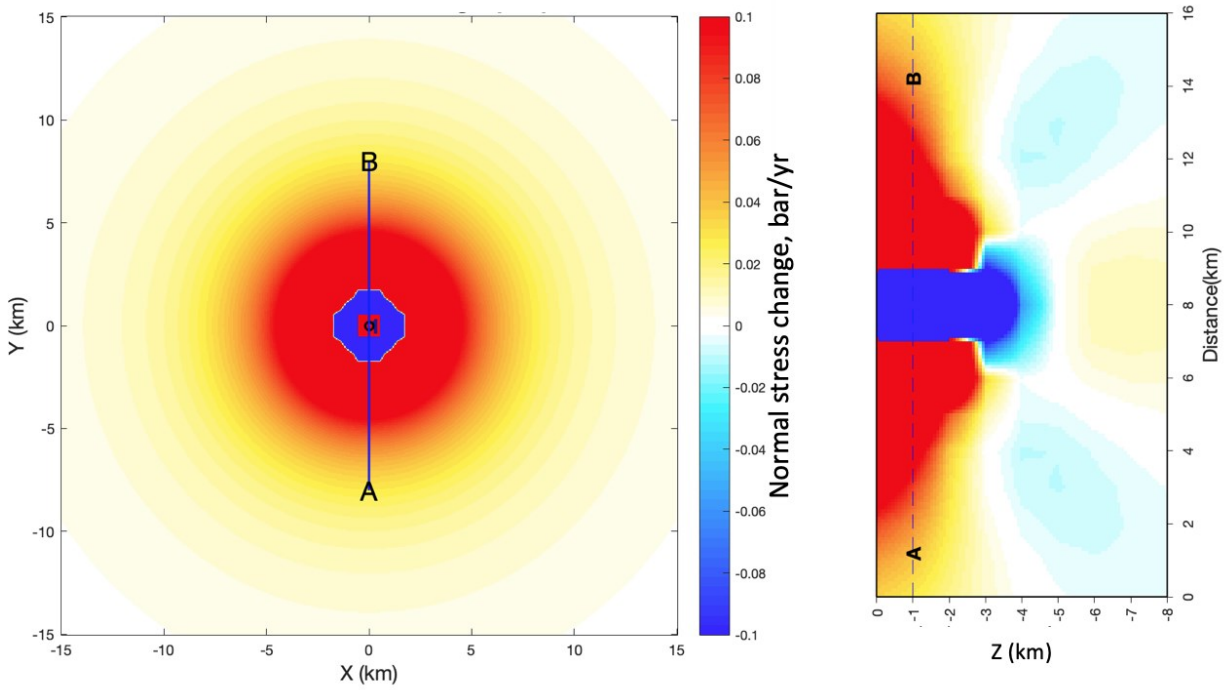

Figure 5: Rate of normal stress change, in bar/yr, with unclamping positive, for a deflating point-source located at 2 km depth. Left: Depth-section at 1 km depth. Right: Cross-sections A-B and C-D as indicated on left figure. The color scale is set to saturate at 0.1 bar/yr.

3.3. Other process interactions

Thermal expansion and contraction cause stress changes in the crust, even well outside the volume where the temperature changes take place. Inside the thermally contracting volume normal stresses are overall reduced, facilitating slip on all fault directions. Outside the contracting volume, the stress changes are identical to what is observed for pressure changes (Figure 4). Thus, the location and temporal changes in microseismicity in geothermal areas may help us to understand whether the deformation process is pressure- or temperature dominated. Deformation at geothermal areas is dominated by pressure-drop in the beginning, but as recharge reaches equilibrium thermal contraction dominates the crustal deformation (e.g., Drouin et al., 2017). In the Húsmúli injection area, it has been observed that lower temperature of wastewater liquids allows for higher injection discharge. This is interpreted as cooling-driven contraction that opens up faults for faster fluid flow (Gunnarsson, 2015).

Chemical alteration and mineralization can also affect stresses, primarily through changes in mechanical properties of rocks and fault gouge. How hydrothermal alteration affects mechanical properties of rocks is quite variable and depends on factors such as parent rocks, pressure and temperature conditions, type of fluid, and duration of water-rock interaction. Poorly consolidated rocks can be strengthened by consolidation, while basaltic and andesitic rocks generally show reduction in strength with alteration, the most extreme weakening with complete alteration to clays (Julia et al., 2014). Clays, especially smectite and illite dominated, have low electrical resistivity (Lévy et al., 2018), such that resistivity measurements have been used to map clay caps indicative of underlying high-temperature geothermal systems (Árnason, 2010; Jousset et al., 2011). Within the geothermal reservoir other clay minerals dominate, such as chlorite and epidote. Juncu et al. (2019) used geodetic measurements from the Hellisheiði geothermal field and poro-elastic models to constrain the bulk modulus of the geothermal reservoir to about 1.3 to 6.4 GPa, significantly less than typically used for crustal rocks, but on par with estimates for e.g. volcanic caldera infills (e.g., Masterlark, 2007).

4. DISCUSSION

The simple stress calculations we present here show how energy production at geothermal areas affects magmatic and tectonic processes far beyond the immediate geothermal area. However, in the geologic long-term, geothermal areas will cool down and contract, so we can argue, to some degree, that the anthropogenic interference is a dramatic speed-up of a natural process. Our models are much simplified from reality, with idealized sources in homogeneous flat-surface media, ignoring various other stress contributions. However, simple stress calculations have been shown to explain triggered seismicity and dike propagation. For example, Feigl et al. (2000) calculated CFS for the 1994-1998 intrusion on optimally oriented faults and found that much of the seismicity occurred in regions of increased CFS. Árnadóttir et al. (2018) used modeling of surface strain to hypothesize that the 2006-present deflation source under Ölkelduháls triggered the 2008 M6.1 earthquake doublet. Segall and Lu (2015) studied how poroealstic effects and time-dependent earthquake nucleation affect earthquake triggering as well. Sigmundsson et al. (2015) used the Bárðarbunga-Holuhraun rifting episode to show how much topographically induced lithostatic stresses can affect the orientation of dike paths. It is thus clear that the calculations presented here are first-order approximations with more detailed stress-driven stories to come.

5. CONCLUSIONS

Stress interactions play an important part for understanding how anthropogenic usage of geothermal energy affects magmatic and tectonic processes. We show that Coulomb Failure Stress changes and normal stress changes grow year-by-year and quickly span areas much greater than the immediate production area.

ACKNOWLEDGEMENTS

This work was supported by the Icelandic Research Fund, grant number 174377-052, and Reykjavík Energy. TerraSAR-X satellite images were acquired through the Supersites initiative. The intermediate TanDEM-X digital elevation model used in the InSAR processing was provided by DLR under project IDEM_GEOL0123.

REFERENCES

Acocella, V.: Structural control on magmatism along divergent and convergent plate boundaries: overview, model, problems, *Earth Sci. Rev*., **136**, (2014), 226e288.

Ali, S. T., et al., Time-series analysis of surface deformation at Brady Hot Springs geothermal field (Nevada) using interferometric synthetic aperture radar, *Geothermics*, **61**, (2016), 114-120.

Árnadóttir, T., Lund, B., Jiang, W., Geirsson, H., Björnsson, H., Einarsson, P., Sigurdsson, T.: Glacial rebound and plate spreading: results from the first countrywide GPS observations in Iceland, *Geophys. J. Int.*, **177**(2), (2009), 691-716.

Árnadóttir, Th., Haines, A. J., Geirsson, H., Hreinsdóttir, S.: A pre-seismic strain anomaly detected before M6 earthquakes in the South Iceland Seismic Zone from GPS station velocities, *J. Geophys. Res.: Solid Earth*, **123**(12), (2018), 11091-11111.

Árnason, K., Eysteinsson, H., Hersir, G. P.: Joint 1D inversion of TEM and MT data and 3D inversion of MT data in the Hengill area, SW Iceland, *Geothermics*, **39**(1), (2010), 13-34,

Bessason, B., Ólafsson, E., Gunnarsson, G., Flovenz, O., Jakobsdóttir, S., Björnsson, S., Árnadóttir, T.: Verklag vegna örvaðrar skjálftavirkni í jarðhitakerfum, Technical Report 2012-24, Orkuveita Reykjavíkur, Reykjavik, Iceland, (2012), 108 pp. (In Icelandic).

Blanck, H., Vogfjörð, K. Geirsson, H.: Mapping and dynamics analysis of fractures in Hengill, SW-Iceland, International Union of Geodesy and Geophysics IUGG, Abstract S01p-370, Montreal, July 2019.

Dahm, T., Cesca, S. Hainzl, S., Braun, T., Krüger, F.: Discrimination between induced, triggered, and natural earthquakes close to hydrocarbon reservoirs: A probabilistic approach based on the modeling of depletion-induced stress changes and seismological source parameters, *J. Geophys. Res. Solid Earth*, **120**, (2015), 2491–2509.

Decriem, J., Árnadóttir, T., Hooper, A., Geirsson, H., Sigmundsson, F., Keiding, M., Ófeigsson, B.G., Hreinsdóttir, S., Einarsson, P., LaFemina, P., Bennett, R. A.: The 2008 May 29 earthquake doublet in SW Iceland, *Geophys. J. Int*., **181**, (2010), 1128–1146.

Drouin, V., Sigmundsson, F., Verhagen, S., Ófeigsson, B. G., Spaans, K., & Hreinsdóttir, S.: Deformation at Krafla and Bjarnarflag geothermal areas, Northern Volcanic Zone of Iceland, 1993–2015, *Journal of Volcanology and Geothermal Research*, ***344***, (2017), 92-105.

Ducrocq, C., Geirsson, H., Árnadóttir, Th., Juncu, D., Drouin, V., Hreinsdóttir, S., Blanck, H., Kristjánsson, B. R., Gunnarsson, G., Ófeigsson, B. G.: The 2017-2018 uplift episode in the Hengill volcanic system, SW Iceland, EGU General Assembly, Abstract EGU2019-14683, Vienna, 7-12 April, (2019).

Einarsson, P., S. Björnsson, G. Foulger, R. Stefánsson, and T. Skaftadóttir: Seismicity pattern in the South Iceland Seismic Zone, in Earthquake Prediction—An International Review, **4**, (1981), 141–151.

Einarsson, P.: Earthquakes and present-day tectonism in Iceland, *Tectonophysics*, **189**, (1991), 261–279.

Einarsson, P., Hjartardóttir, Á. R., Hreinsdóttir, S., & Imsland, P.: The structure of seismogenic strike-slip faults in the eastern part of the Reykjanes Peninsula Oblique Rift, SW Iceland, *Journal of Volcanology and Geothermal Research*, in press, (2018).

Feigl, K. L., Gasperi, J., Sigmundsson, F. & Rigo, A.: Crustal deformation near Hengill volcano, Iceland 1993–1998: coupling between magmatic activity and faulting inferred from elastic modeling of satellite radar interferograms, *Journal of Geophysical Research: Solid Earth,* **105**, (2000), 25655-25670.

Flóvenz, Ó. G., K. Ágústsson, E. Á. Guðnason, S. Kristjánsdóttir: Reinjection and Induced Seismicity in Geothermal Fields in Iceland. World Geothermal Congress 2015, Melbourne, Australia, 19-24 April, (2015), 15 pp.

Geirsson, H., Árnadóttir, T., Völksen, C., Jiang, W., Sturkell, E., Villemin, T., Einarsson, P. & Sigmundsson, F.: Current plate movements across the Mid-Atlantic ridge determined from 5 years of continuous GPS measurements in Iceland, *Journal of Geophysical Research: Solid Earth,* 111, (2006), B09407.

Geirsson, H., et al.: Overview of results from continuous GPS observations in Iceland from 1995 to 2010, *Jökull*, **60**, (2010), 3-22.

Geirsson, H., et al.: Volcano deformation at active plate boundaries: Deep magma accumulation at Hekla volcano and plate boundary deformation in south Iceland, *J. Geophys. Res*., **117**, (2012), B11409.

Gudmundsson, A., and Philipp, S. L.: How local stress fields prevent volcanic eruptions. *Journal of Volcanology and Geothermal research,* **158**(3-4), (2006), 257-268.

Gunnarsson, G., Kristjánsson, B. R., Gunnarsson, I., Júlíusson, B. M.: Reinjection into a Fractured Reservoir – Induced Seismicity and Other Challenges in Operating Reinjection Wells in the Hellisheiði Field, SW-Iceland, World Geothermal Congress, (2015), Melbourne, Australia, 19-24 April, 9 pp.

Harris, R. A., Simpson, R. W.: Changes in static stress on southern California faults after the 1992 Landers earthquake, *Nature*, **360**, (1992), 313-318.

Hooper, A.: A multi-temporal insar method incorporating both persistent scatterer and small baseline approaches, *Geophys. Res. Lett.,* **35**, (2008), L16302.

Hooper, A., Bekaert, D., Spaans, K., Arıkan, M.: Recent advances in SAR interferometry time series analysis for measuring crustal deformation, *Tectonophysics*, **514**, (2012), 1–13.

Hreinsdóttir, S., Árnadóttir, T., Decriem, J., Geirsson, H., Tryggvason, A., Bennett, R. A., LaFemina, P.: A complex earthquake sequence captured by the continuous GPS network in SW Iceland, *Geophys. Res. Lett*., **36**, (2009), L12309.

Im, K., Elsworth, D., Guglielmi, Y., & Mattioli, G. S.: Geodetic imaging of thermal deformation in geothermal reservoirs - production, depletion and fault reactivation, *Journal of Volcanology and Geothermal Research*, **338**, (2017), 79-91.

Jakobsdóttir, S. S.: Seismicity in Iceland: 1994–2007, *Jökull,* **58**, (2008), 75-100.

Jousset, P., Haberland, C., Bauer, K., Arnason, K.: Hengill geothermal volcanic complex (Iceland) characterized by integrated geophysical observations, *Geothermics*, **40**(1), (2011), 1–24.

Jónsson, S., Segall, P., Pedersen, R., Björnsson, G.: Post-earthquake ground movements correlated to pore-pressure transients, *Nature*, **424**, (2003), 179–183.

Julia, F., Vladimir, L., Sergey, R., & David, Z.: Effects of hydrothermal alterations on physical and mechanical properties of rocks in the Kuril–Kamchatka island arc, *Engineering geology*, **183**, (2014), 80-95.

Juncu, D., Árnadóttir, Th., Hooper, A., Gunnarsson G.: Anthropogenic and natural ground deformation in the Hengill geothermal area, Iceland, *Journal of Geophysical Research: Solid Earth,* **122**(1), (2017): 692-709.

Juncu, D., Árnadóttir, Th., Geirsson, H., Guðmundsson, G. B., Lund, B., Gunnarsson, G., Hooper, A., Hreinsdóttir S., Michalczewska K.: Injection-induced surface deformation and seismicity at the Hellisheidi geothermal field, Iceland, *Journal of Volcanology and Geothermal Research*, in press, (2018).

Juncu, D., Árnadóttir, Th., Geirsson, H., Gunnarsson, G.: The effect of fluid compressibility and elastic rock properties on deformation of geothermal reservoirs, *Geophysical Journal International*, **217**(1), (2019), 122-134.

Kampes, B. M., Hanssen, R. F., Perski, Z.: Radar interferometry with public domain tools, 3rd International Workshop on ERS SAR Interferometry, 'FRINGE03', Frascati, Italy, (2003), p. 6.

LaFemina, P.: Plate tectonics and volcanism, *Encyclopedia of Volcanoes*, 2nd edition, (2015), 65-92.

La Femina, P. C., Connor, C. B., Hill, B. E., Strauch, W., & Saballos, J. A.: Magma–tectonic interactions in Nicaragua: the 1999 seismic swarm and eruption of Cerro Negro volcano, *Journal of Volcanology and Geothermal Research*, **137**(1-3), (2004), 187-199.

LaFemina, P. C., Dixon, T.H., Malservisi, R., Árnadóttir, T., Sturkell, E. Sigmundsson, F. & Einarsson, P.: Geodetic GPS measurements in south Iceland: strain accumulation and partitioning in a propagating ridgesystem, *Journal of Geophysical Research: Solid Earth,* **110**, (2005), B11405.

Lévy, L., Gibert, B., Sigmundsson, F., Flóvenz, Ó. G., Hersir, G. P., Briole, P., & Pezard, P. A.: The role of smectites in the electrical conductivity of active hydrothermal systems: electrical properties of core samples from Krafla volcano, Iceland, *Geophysical Journal International,* **215**(3), (2018), 1558-1582.

Massonnet, D., Feigl, K. L.: Discrimination of geophysical phenomena in satellite radar interferograms, *Geophys. Res. Lett*., **22**(12) (1995), 1537-1540.

Masterlark, T.: Magma Intrusion and deformation predictions: Sensitivities to the Mogi assumptions, *J. Geophys. Res*., **112**, (2007), B06419.

Nostro, C., Stein, R.S., Cocco, M., Belardinelli, M. E., and Marzocchi, W.: Two-way coupling between Vesuvius eruptions and southern Apennine earthquakes (Italy) by elastic stress transfer, *Journal of Geophysical Research*, **103**, (1998), 24487-24504.

Segall, P., & Lu, S.: Injection-induced seismicity: Poroelastic and earthquake nucleation effects, *Journal of Geophysical Research: Solid Earth*, **120**(7), (2015), 5082-5103.

Sigmundsson, F., Einarsson, P., Bilham, R., Sturkell, E.: Rift-transform kinematics in south Iceland: deformation from Global Positioning System measurements, 1986 and 1992, *Journal of Geophysical Research*, **100**, (1995), 6235-6248.

Sigmundsson, F., Einarsson, P., Røgnvaldsson, S. T., Foulger, G. R., Hodgkinson, K. M., Thorbergsson, G.: The 1994–1995 seismicity and deformation at the Hengill triple junction, Iceland: triggering of earthquakes by minor magma injection in a zone of horizontal shear stress, *Journal of Geophysical Research,* **102**, (1997), 15151-15161.

Sigmundsson, F., et al.: Segmented lateral dyke growth in a rifting event at Bárðarbunga volcanic system, Iceland, *Nature*, **517**(7533), (2015), 191.

Sigmundsson, F., Einarsson, P., Hjartardóttir, Á. R., Drouin, V., Jónsdóttir, K., Árnadóttir, Th., Geirsson, H, Hreinsdóttir, S., Li, S., Ófeigsson, B. G.: Geodynamics of Iceland and the signatures of plate spreading, *Journal of Volcanology and Geothermal Research*, in press, (2018).

Steigerwald, L., Einarsson, P., Hjartardóttir, Á. R.: Fault kinematics at the Hengill Triple Junction, SW-Iceland, derived from surface fracture pattern, *Journal of Volcanology and Geothermal Research*, in press, (2018).

Stein, R. S.: The role of stress transfer in earthquake occurrence, *Nature*, **402**(6762), (1999), 605-609.

Stimac, J., Goff, F., Goff, C. J.: Intrusion-related geothermal systems, *The Encyclopedia of Volcanoes*, Academic Press, (2015), 799-822.

Toda, S., Stein, R. S., Sevilgen, V., Lin, J.: Coulomb 3.3 graphic-rich deformation and stress-change software for earthquake, tectonic, and volcano research and teaching-user guide, US Geological Survey, technical report No. 2011-1060, 2011.

Vogfjörd, K., Slunga, R.: Rupture in the South Iceland Seismic Zone forced by magmatic intrusion in the Hengill area, EGS-AGU-EUG Joint Assembly, **1**, (2003), pp. 9685.